ORIGINAL ARTICLE

Cancer Science WILEY

S-1 eliminates MDSCs and enhances the efficacy of PD-1 blockade via regulation of tumor-derived Bv8 and S100A8 in thoracic tumor

Na T. Nguyen[1] | Atsushi Mitsuhashi[1] | Hirokazu Ogino[1] | Hiroyuki Kozai[1] | Hiroto Yoneda[1] | Tania Afroj[1] | Seidai Sato[1] | Hiroshi Nokihara[1] | Tsutomu Shinohara[2] | Yasuhiko Nishioka[1,3]

[1]Department of Respiratory Medicine and Rheumatology, Graduate School of Biomedical Sciences, Tokushima University, Tokushima, Japan

[2]Department of Community Medicine for Respirology, Graduate School of Biomedical Sciences, Tokushima University, Tokushima, Japan

[3]Department of Community Medicine for Rheumatology, Graduate School of Biomedical Sciences, Tokushima University, Tokushima, Japan

Correspondence
Yasuhiko Nishioka, Department of Respiratory Medicine and Rheumatology, Graduate School of Biomedical Sciences, Tokushima University, 3-18-15 Kuramoto-cho, Tokushima 770-8503, Japan.
Email: yasuhiko@tokushima-u.ac.jp

Funding information
Japan Society for the Promotion of Science (JSPS), Grant/Award Number: 19H03668; Taiho Pharmaceutical

Abstract

Myeloid-derived suppressor cells (MDSCs) have been known to play a pivotal role in the induction of immune tolerance, which limits the benefits of immune check-point inhibitors (ICIs). Recent studies revealed that several chemotherapeutic agents decreased tumor-infiltrating MDSCs. Therefore, combination therapy with cytotoxic chemotherapeutic agents and ICIs was approved for first-line treatment for lung cancer. However, the impact of chemotherapeutic agents on MDSCs and an optimal partner of ICIs has not been fully investigated in thoracic tumors, including lung cancer and malignant pleural mesothelioma. In the present study, we found that treatment with 5-FU and its oral formulation, S-1, suppressed tumor progression and inhibited the accumulation of MDSCs in thoracic tumor-bearing mice. Tumor-infiltrating T cells and dendritic cells were significantly expanded in S-1-treated mice. 5-FU suppressed the ability of tumor cells to recruit MDSCs, while it did not suppress the survival and differentiation of mouse MDSCs in vitro. We also revealed that 5-FU or S-1 significantly downregulated the expression of tumor-derived Bv8 and S100A8. The knockdown of Bv8 or S100A8 in tumor cells suppressed tumor growth and MDSC recruitment in vivo. Furthermore, in comparison with pemetrexed, administration of S-1 improved the synergistic therapeutic efficacy of anti-PD-1 antibodies with or without carboplatin. Our findings revealed a novel mechanism wherein S-1 primed a favorable tumor microenvironment to provide the rationale for combination therapy with S-1 and ICIs as the optimal therapy for thoracic cancer.

KEYWORDS
Bv8, immune checkpoint inhibitor, myeloid-derived suppressor cells, S-1, S100A8

1 | INTRODUCTION

Thoracic malignant tumors, including lung cancer and malignant pleural mesothelioma (MPM) are the leading cause of cancer-related deaths worldwide.[1,2] Immune checkpoint inhibitors (ICIs) targeting programmed death 1 (PD-1) and its ligand PD-L1, play a vital role in T-cell tolerance to provide significant clinical benefits in various solid tumors, including lung cancer, colorectal cancer, and head and neck cancer.[3–5] In addition, recent clinical trials demonstrated that cytotoxic chemotherapeutic agents enhanced the clinical benefit of ICIs. Thus, combination therapy with ICI and platinum plus either pemetrexed (PEM) or taxane was approved for the first-line treatment of non–small-cell lung cancer (NSCLC).[6,7] Although combination immunotherapy improved the outcomes of malignancies, the optimum regimen has not been fully identified.

Myeloid-derived suppressor cells (MDSCs) are known as a heterogeneous population of cells originating from bone marrow. MDSC populations are characterized as $CD11b^+Gr-1^+$ in mice. MDSCs play a vitally important role in facilitating tumor invasion, metastasis, and angiogenesis. MDSCs are also known to inhibit antitumor immunity via the suppression of cytotoxic functions of T cells, natural killer cells, and stimulating regulatory T cells.[8–10] Recent studies revealed that MDSCs have a potential application as a prognostic marker for the ICI response.[8,11–13] Accordingly, the expansion of MDSCs was found to be correlated with the clinical response in melanoma patients treated with ipilimumab[14] and lung cancer with anti-PD-1 antibody.[13,15] Thus, the combination of MDSC targeting therapy and ICIs could be a promising cancer treatment strategy.

Several studies have demonstrated that 5-fluorouracil (5-FU) reduced tumor-infiltrating MDSCs in a preclinical model.[16,17] As for thoracic tumors, an oral fluoropyrimidine agent that contains tegafur, a prodrug of 5-FU, with gimeracil and oteracil potassium (S-1) showed a clinical benefit.[18–20] Currently, S-1 has marked antitumor effects on lung cancer[20–22] and mesothelioma.[23] Nevertheless, the influence of S-1 on tumor-infiltrating MDSCs remains unclear.

In this study, we evaluated the effects of chemotherapeutic agents approved for patients with thoracic tumors on tumor-associated MDSCs in vivo. We found that S-1 significantly reduced the infiltration of MDSCs and promoted tumor-infiltrating T-lymphocytes (TILs) and dendritic cells (DCs) in syngeneic mouse models. The present study indicated that the administration of S-1, but not PEM, is the best option to combine with ICIs, and improved the antitumor efficacy in vivo. In addition, the mechanisms through which S-1 suppressed the recruitment of MDSCs were investigated.

2 | MATERIALS AND METHODS

2.1 | Cell lines

The mouse mesothelioma cell line, AB1-HA, was purchased from Public Health England. The mouse lung cancer cell line, 3LL, was purchased from ATCC. 293FT producer cells for the production of lentiviral particles were purchased from ATCC. AB1-HA and 3LL were cultured in DMEM (Gibco) and supplemented with 10% heat-inactivated FBS (Merck) and 1% penicillin/streptomycin (P/S; Meiji Seika) at 37°C under 5% CO_2. 3LL was incubated in RPMI 1640 medium (Gibco) with 10% FBS and P/S.

2.2 | Animal models

Five-week-old male BALB/c and C57BL/6 mice were purchased from the Charles River Laboratories. AB1-HA cells or 3LL cells were subcutaneously injected into the flanks of BALB/c mice or C57BL/6 mice (1×10^6 cells/100 μl PBS), respectively. In the lung metastasis model, 3LL cells (5×10^5 cells/200 μl PBS) were injected into tail veins. To evaluate the efficacy of chemotherapy, mice were treated by intraperitoneal injection of PEM (100 mg/kg), 5-FU (80 mg/kg), carboplatin (CBDCA; 50 mg/kg), cisplatin (CDDP; 3 mg/kg), vinorelbine (VNR; 10 mg/kg), paclitaxel (PTX; 30 mg/kg), docetaxel (DOC; 40 mg/kg), or gemcitabine (GEM, 120 mg/kg) on day 14 or daily oral gavage S-1 (8.3 mg/kg/day) from day 14 to day 20. The dose of chemotherapeutic drugs was determined according to the maximum tolerated dose (MTD) reported in a previous study.[24] S-1 was purchased from Taiho Pharmaceutical Co., Ltd. The other chemotherapeutic agents were purchased from Selleck Chem.

To determine the impact of combination treatment with ICIs, anti-PD-1 antibody (100 μg/mouse/day) or isotype control rat IgG2a (100 μg/mouse/day) were administered twice a week. Anti-PD-1 monoclonal antibody (RMP1-14) and isotype control IgG were purchased from BioXCell. To deplete MDSC, the mice were treated with anti-Gr-1 antibody (100 μg/mouse/day) or isotype control rat IgG2b (100 μg/mouse/day) twice a week, which were purchased from BioXCell.

Mice were maintained under specific-pathogen-free conditions. All animal experiments were performed in accordance with the guidelines established by the Tokushima University Committee on Animal Care and Use. At the end of each in vivo experiment, mice were anesthetized with isoflurane and euthanized humanely by cutting the subclavian artery. The tumor size was measured twice a week, where volume $= ab^2\,2^{-1}$ (a, long diameter; b, short diameter).

2.3 | Cell viability assay

AB1-HA or 3LL cells were seeded into 96-well plates (2×10^3 cells/100 μl/well) the day before treatment. Following treatment with different concentrations of 5-FU or PEM for 72 h, 50 μl of MTT solution [2 mg/ml; 3-(4,5-dimethylthiazol–2-yl)-2,5-diphenyl tetrazolium bromide; Sigma] was added to each well and incubated for 3 h at 37°C. The MTT-containing medium was discarded, and the dark blue crystals were dissolved by adding 100 μl of DMSO (Wako). The absorbance was read using a SUNRISE Remote R microplate reader (Tecan) at 450 nm and reference wavelengths of 630 nm. AB1-HA tumor-bearing mice were sacrificed and their

spleens were harvested. MDSCs were isolated from splenocytes using a mouse Myeloid-Derived Suppressor Cell Isolation Kit (Miltenyi Biotec) according to the manufacturer's instructions. After seeding MDSCs (2×10^3 cells/100 μl/well) into a 96-well plate the day before treatment, cells were treated with different concentrations of 5-FU for 72 h and then incubated for 3 h with CCK-8 reagent (DingGuo Bio) at 37°C. We measured the absorbance at 450 nm with a SUNRISE Remote R microplate reader. The half-maximal inhibitory concentration (IC_{50}) was calculated using GraphPad Prism 5 software.

2.4 | Quantitative real-time PCR

Tumor cell lines were seeded into 24-well plates and incubated 1 day before treating with IC_{50} of 5-FU or PEM for 48 h at 37°C. Tumor tissues were collected from AB1-HA- or 3LL-bearing mice treated with S-1 or PEM. Total RNA was extracted using an RNeasy Mini Kit (Qiagen) according to the manufacturer's instructions. After detection of the RNA concentration, cDNA synthesis was performed with 2 μg RNA using a high-capacity RNA-to-cDNA kit (Thermo Fisher Scientific). TB Green Premix Ex Taq™ (TaKaRa) was used for qRT-PCR with the C1000TM Thermal Cycler machine. The specific primers were purchased from Eurofins Genomics. Mouse RPS29 mRNA was used as a housekeeping gene and relative mRNA levels were determined using the $\Delta\Delta C_t$ method. The primer sequences are shown in Table S1.

2.5 | Flow cytometry

Splenocytes were gently crushed through a 70-μm cell strainer followed by RBC lysis. Tumor fragments were cut into small pieces with scissors and then digested by digestion buffer consisting of 1 mg/ml BSA (Sigma-Aldrich), 1 mg/ml collagenase IV (ThermoFisher Scientific), and 100 μg/ml DNase I (Roche) in DMEM for 1-h incubation at 37°C, followed by passaging through a 100-μm cell strainer. To examine the differentiation of bone marrow cells to MDSCs in vitro, bone marrow cells were isolated from 7-week-old BALB/c mice and 3×10^6 cells were cultured for 3 days in RPMI-1640 medium containing 10% FBS, 10 ng/ml GM-CSF, 10 ng/ml IL-4 and 0.2 ng/ml TGF-β (PeproTech). Single-cell suspensions from tumors, spleens, and bone marrow cells were centrifuged and saturated with FACS buffer (PBS containing 0.5% FBS). The cells were incubated with FcR blocking reagent (BD Biosciences) and the following antibodies for 30 min on ice in 96 V-bottomed well plates: phycoerythrin (PE)-conjugated anti-Gr1, fluorescein isothiocyanate (FITC)-conjugated anti-CD11b, PE-conjugated anti-CD8a, FITC-conjugated anti-CD4, PE-conjugated anti-Ly6G, and PE-Cy7-conjugated anti-Ly6C. All antibodies were purchased from BD Biosciences. Cells were then washed with FACS buffer and fixed with 2% formalin/PBS before analyzing

by flow cytometry. The FlowJo_v10.6.0 software program (BD Biosciences) was used for the analysis.

2.6 | Immunofluorescence

Frozen sections of resected tumors were cut into 8-μm serial slices. Slices were fixed in 4% paraformaldehyde for 5 min at room temperature, followed by serum-free blocking protein (Dako). Samples were subsequently stained with primary antibodies, such as anti-CD4 (1:50; BD Pharmingen), anti-CD8 (1:150; BD Pharmingen), anti-PD-1 (1:100; Abcam), anti-Foxp3 (1:400; Novus Biologicals) and anti-dendritic cell marker which reacts with dendritic cell inhibitory receptor 2 (1:50; Novus Biologicals), and anti-Gr-1 (1:100; BD Pharmingen) antibodies overnight at 4°C. After washing, fluorescence-labeled secondary antibodies (Alexa Fluor 594 goat anti-rat, Alexa Fluor 488 goat anti-rabbit and Alexa Fluor 488 donkey anti-goat IgG H+L [1:250, Life Technologies]) were then applied to the sections for 30 min at room temperature. DAPI (Vector Laboratory) was used for nuclear staining. Stained slides were finally imaged using an Olympus BX61 scanning fluorescence microscope. For quantification data, counting was performed in three random fields at ×200 magnification per tumor tissue specimen.

2.7 | Western blotting

AB1-HA cells were treated or untreated with IC_{50} of 5-FU (1 μM) for 24 h; 48 h or 72 h at 37°C, followed by homogenization in M-PER reagents (Thermo Fisher) containing phosphatase and protease inhibitor cocktails (Roche). Protein concentrations were determined using a TaKaRa Bradford Protein Assay kit (Takara) and read at 450 nm with a SUNRISE Remote R microplate reader (Tecan). The protein lysates were transferred to polyvinylidene fluoride membrane and blocked by blocking one solution for 1 h (Nacalai Tesque) The membranes were incubated overnight at 4°C with primary antibodies (dilution: 1:1000) to S100A8 (Cell Signaling Technology), Bv8 (Abcam) and β-actin (Santa Cruz Biotechnology). After washing, membranes were applied using horseradish peroxidase (HRP)-conjugated secondary antibodies (GE Healthcare), and visualized through a chemiluminescent Amersham Imager 600 machine.

2.8 | Migration assay

MDSC migration was assessed using a 5 μm pore size transwell (Costar). AB1-HA cells were cultured in 0.1% FBS containing-DMEM with or without 5-FU (1 μM) for 48 h. The cell culture supernatant was applied to the lower chamber. Mouse splenic MDSCs (5×10^5 cells/100 μl) were seeded in the upper chamber. After 6 h, the membranes were fixed and stained using a Diff-Quik stain kit (Sysmex). The cells that had migrated to the bottom surface of the

filter were counted in six randomly selected fields on each filter under a microscope at ×200 magnification.

2.9 | Lentiviral transduction

Lentiviral shRNA pLKO.1 constructs (Sigma-Aldrich) were used to make self-inactivating shRNA lentivirus for Bv8 (TRCN0000104997), S100A8 (TRCN0000104759) and a non-target random scrambled sequence control. To harvest the lentiviral particles, shRNA was co-transfected with MISSION Lentiviral Packaging Mix (Sigma-Aldrich) in packaging cells (293FT) using FuGENE 6 (Roche). For virus transduction, 2.0×10^6 AB1-HA cells were incubated with lentivirus for 24 h. The successfully transduced clones were identified by 10 μg/ml puromycin (Sigma-Aldrich) selection. To evaluate the cell proliferation in vitro, transfected AB1-HA cells were cultured for 4 days in 96-well plate, followed by daily cell proliferation assay using MTT solution. To examine the influence of Bv8 and S100A8 on tumor progression, Bv8 or S100A8-targeting shRNA expressing-AB1-HA cells were subcutaneously implanted into the flank of BALB/c mice. Control shRNA expressing AB1-HA cell-bearing mice were treated with or without daily oral gavage of S-1 (8.3 mg/kg/day) from day 7 to 13.

2.10 | Statistical analysis

GraphPad Prism 5 software was used to analyze the data. Data were analyzed using Student's *t*-test for unpaired samples, the Mann–Whitney *U*-test, or a one-way ANOVA, followed by Tukey's multiple-comparison post-hoc test, as appropriate. Significance levels are indicated with asterisks in the figures and were as follows: ns, not statistically significant, $*p < 0.05$, $**p < 0.01$, $***p < 0.001$, and $****p < 0.0001$.

3 | RESULTS

3.1 | Fluoropyrimidines suppress tumor progression and MDSC accumulation in thoracic tumor-bearing mice

Recent studies revealed that some chemotherapeutic agents, such as 5-FU and GEM, reduced tumor-infiltrating MDSCs in solid tumors.[16,17,25] Using AB1-HA cells, a mouse mesothelioma cell line, we focused on the capacity of various chemotherapeutic reagents approved for thoracic tumors to reduce MDSCs in vivo. AB1-HA-bearing mice received a single intraperitoneal administration of PEM, 5-FU, carboplatin (CBDCA), cisplatin (CDDP), vinorelbine (VNR), paclitaxel (PTX), docetaxel (DOC) and gemcitabine (GEM) on day 14 or oral gavage of S-1 from day 14 to 20 after tumor inoculation. The number of CD11b$^+$,Gr-1$^+$ MDSCs was evaluated at 21 days after tumor inoculation by flow cytometry. Although GEM and CBDCA reduced tumor progression, there was no difference in the MDSCs in tumor tissue (Figure S1A–F). Even though combination

immunotherapy with PEM or taxane was approved for the standard treatment of NSCLC, PEM and PTX failed to suppress tumor growth and the accumulation of MDSCs (Figure 1A–C and Figure S1A). Only 5-FU and S-1 were able to suppress tumor growth (Figure 1B) and the accumulation of MDSCs in both the spleen and tumor tissue (Figure 1C–F). To examine the roles of MDSCs in tumor progression, we compared antitumor effects of S-1 and anti-Gr-1 antibody in AB1-HA tumor-bearing mice (Figure S1G,H). The antitumor effects of S-1 and MDSC depletion were same extent in vivo. These results indicated that MDSCs play pivotal roles in tumor progression. We immunohistochemically analyzed the number of Gr-1$^+$ MDSCs in the tumor microenvironment (Figure 1G,H). Tumor-infiltrating MDSCs were significantly reduced by S-1, but not PEM. We found similar results using the 3LL model (Figure S2A–D). To determine whether S-1 eliminates the tumor-infiltrating MDSCs in the lung microenvironment, we performed lung metastasis model (Figure S2E,F). S-1 also decreased the number of MDSCs in lung metastatic foci. MDSCs can be subdivided into two major subsets, polymorphonuclear MDSC (PMN-MDSC) and monocytic MDSC (M-MDSC).[8] S-1 dramatically decreased both M-MDSCs (CD11b$^+$Ly6C^{high}Ly6G$^-$) and PMN-MDSCs (CD11b$^+$Ly6C^{low}Ly6G$^+$) in spleens (Figure 1I). However, only M-MDSC was significantly suppressed in tumor tissue after S-1 treatment (Figure 1J). Thus, these results indicated that fluoropyrimidines effectively inhibited tumor progression and MDSC infiltration in thoracic tumor-bearing hosts among nine cytotoxic agents approved for thoracic cancer.

3.2 | S-1 induces the increase of antitumor immune cells in mesothelioma tumor-bearing mice

MDSCs have been known to induce immune tolerance by regulating multiple tumor-associated immune cells, such as T cells, dendritic cells, and regulatory T cells.[26] To investigate whether S-1 induced antitumor immunity via the suppression of MDSCs, we evaluated the effects of S-1 or PEM treatment on the tumor-infiltrating T-cell population and dendritic cells. In comparison with control mice, S-1 significantly enhanced the frequency of CD4$^+$ and CD8$^+$ T cells in the spleen (Figure S3A,B). S-1 markedly increased the number of CD4$^+$ T cells, CD8$^+$ T cells, and dendritic cells in tumor tissue, while PEM did not (Figure 2A–C). We found that S-1 did not induce the expansion of regulatory T cells (Figure S3C). S-1 decreased the percentage of PD-1$^+$CD8$^+$ exhausted T cells (Figure S3D) and increased the expression of granzyme B in tumor microenvironment (Figure S3E). These results suggested that S-1 treatment enhanced antitumor immunity by inhibiting the accumulation of MDSCs.

3.3 | Fluoropyrimidines inhibit the accumulation of MDSCs via the downregulation of tumor-derived soluble factors

In tumor-bearing mice, MDSCs are mainly generated in the bone marrow and arrest in the spleen, then mobilize to the tumor
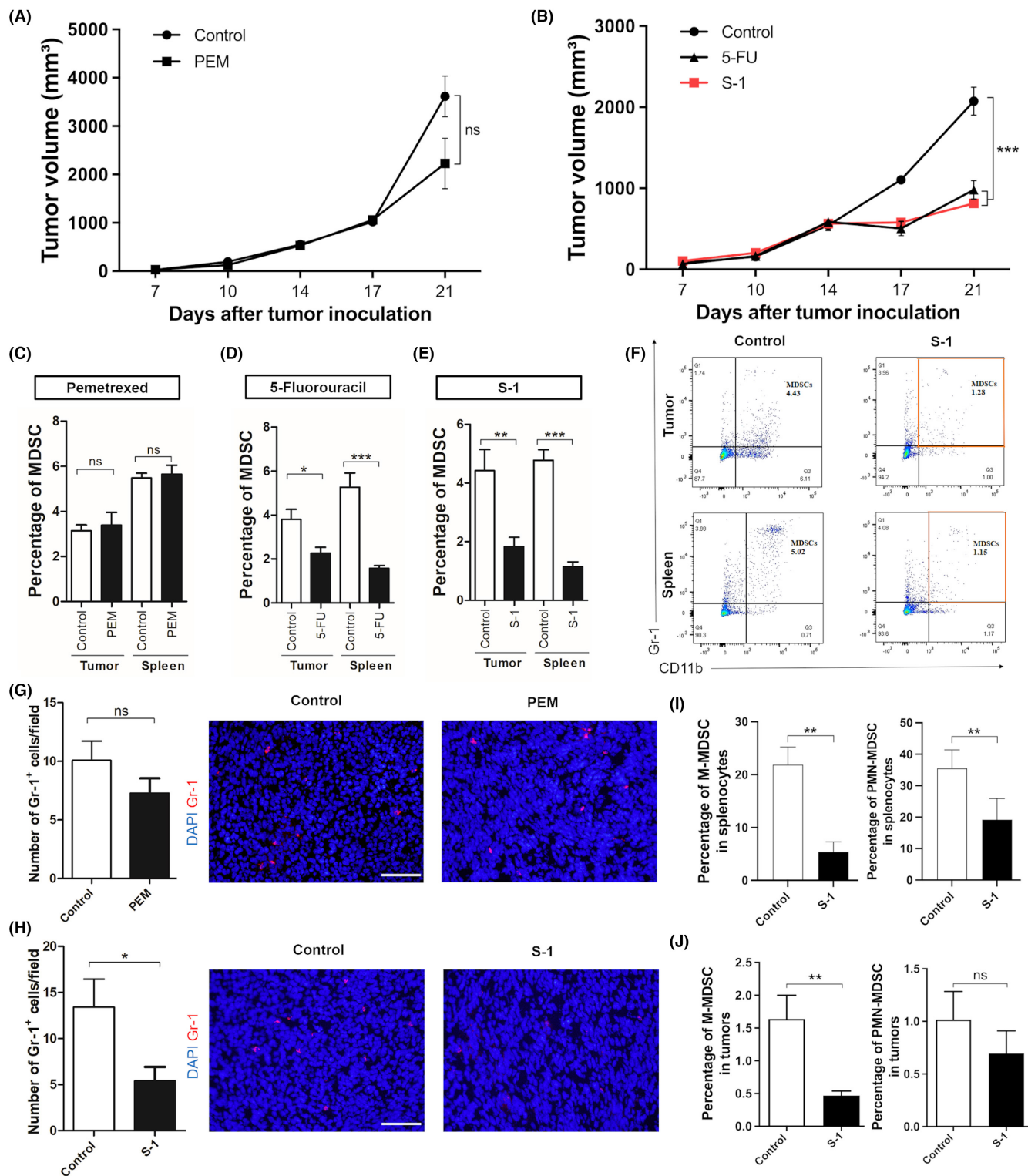
FIGURE 1 Fluoropyrimidines suppress tumor progression and MDSC accumulation. (A, B) Evaluation of the tumor volume of AB1-HA tumor-bearing mice treated with S-1 (o.g., daily from day 14 to 20) or PEM (i.p., day 14) or 5-FU (i.p., day 14). (C–F) Flow cytometry of $CD11b^+Gr-1^+$ MDSCs in tumor tissue and spleen derived from AB1-HA tumor-bearing mice treated with PEM (C), 5-FU (D), or S-1 (E, F) on day 21 ($n = 10$ per group). (G, H) Representative images and the quantitative evaluation of $Gr-1^+$ cells in each field in tumor tissue specimens from AB1-HA tumor-bearing mice treated with S-1 (G) or PEM (H), $n = 5$ per group. Scale bars, 200 μm. (I, J) Flow cytometry of $CD11b^+Ly6C^{high}Ly6G^-$ M-MDSCs and $CD11b^+Ly6C^{low}Ly6G^+$ PMN-MDSCs in spleens (I) or in tumors (J) derived from AB1-HA tumor-bearing mice treated with S-1, $n = 6$ per group. Data are shown as the mean ± SEM of two independent experiments: ***$p < 0.001$; **$p < 0.01$; *$p < 0.05$; ns, not statistically significant by Mann–Whitney U-test or one-way ANOVA. i.p., intraperitoneal; o.g., oral gavage.

FIGURE 2 S-1 induces the increase in tumor-infiltrating immune cells in mesothelioma tumor-bearing mice. The immunofluorescence analysis of CD8, CD4, and DC markers in the tumor tissues of AB1-HA-bearing mice treated with PEM or S-1. Representative images and quantitative evaluation of the number of (A) $CD8^+$ cells, (B) $CD4^+$ cells, and (C) Dendritic Cell Inhibitory Receptor 2 (DCIR2) on dendritic cells per field ($n = 5$ per group). Scale bars, 200 μm. Data are shown as the mean ± SEM. **$p < 0.01$; *$p < 0.05$; ns, not statistically significant by Mann–Whitney U-test.
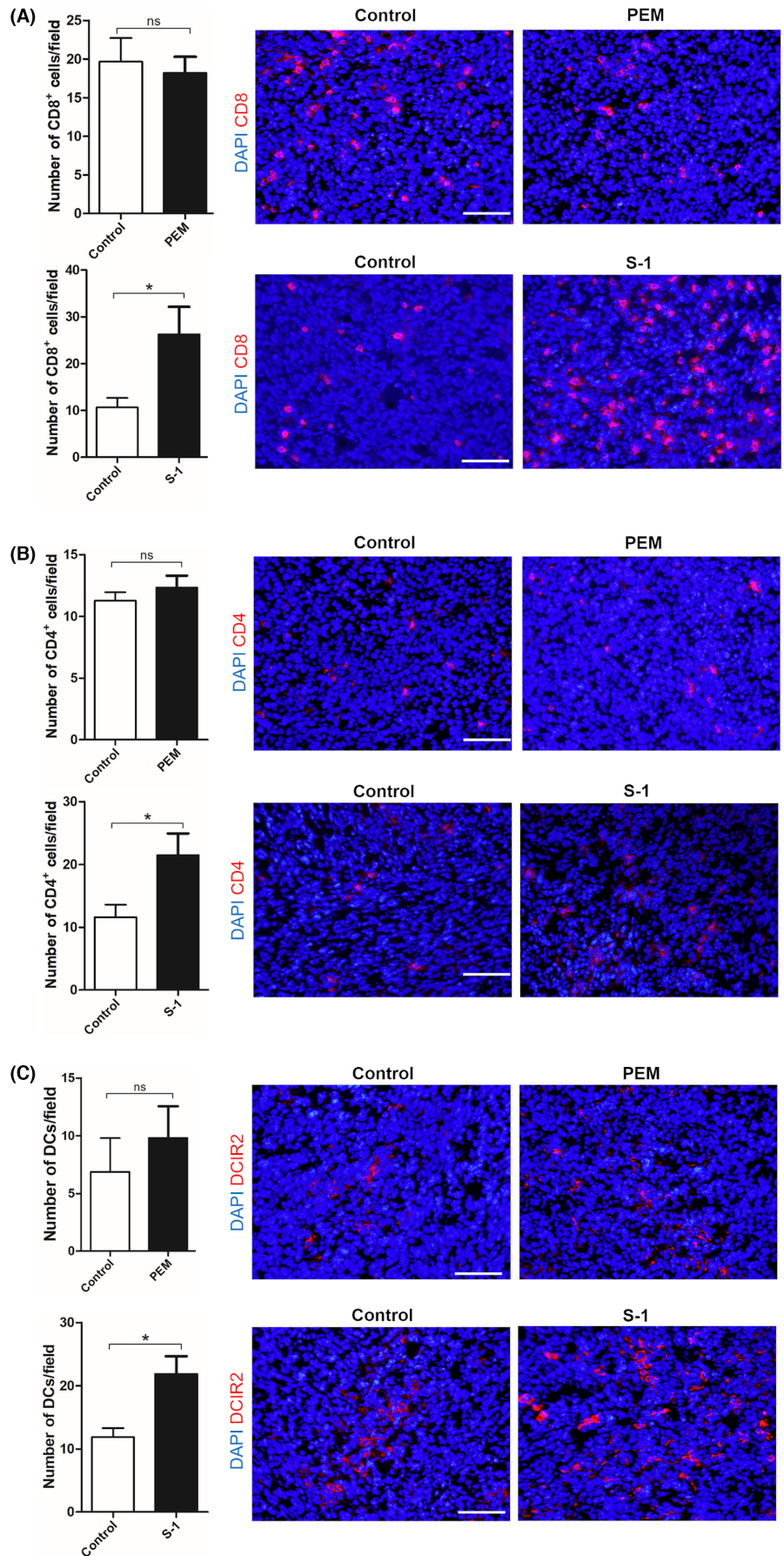
microenvironment.[27] To determine whether 5-FU and its oral formulation (S-1) treatment regulated the recruitment or survival of MDSC, we evaluated the cytotoxicity of 5-FU on MDSCs and AB1-HA tumor cells. Spleen-derived murine MDSCs, or AB1-HA tumor cells were incubated with or without 5-FU. We revealed that while 5-FU induced direct cytotoxic effects on tumor cells, it had no significant effect on the cell viability of MDSCs (Figure 3A,B). In addition, 5-FU treatment did not inhibit the differentiation of mouse bone marrow cells to MDSCs in vitro (Figure 3C). Taken together, we focused on the effects of fluoropyrimidines on the MDSC-recruitment capacity of tumor cells. By performing a migration assay, we found that conditioned medium from AB1-HA cells treated with 5-FU, reduced the number of migrating MDSCs in comparison with non-treated tumor cells (Figure 3D). These results indicated that S-1 did not suppress the cell viability or differentiation of MDSCs, but regulated tumor cell-dependent MDSC recruitment.

Tumor-derived soluble factors are known to play a critical role in the recruitment of MDSCs to the tumor microenvironment.[27–29] Therefore, we next evaluated the possibility that S-1 and 5-FU modified tumor cell-derived mediators in vivo and in vitro, respectively. We examined the gene expression levels of chemokines and cytokines involved in MDSC recruitment. 5-FU treatment (in vitro) and S-1 treatment (in vivo) induced the downregulation of S100A8, Bv8, and iNOS, while PEM did not suppress these MDSC-associated factors (Figure 4A–D). Moreover, S-1 upregulated the IFNγ expression in vivo (Figure 4A), reflecting the increase of TILs. Bv8 and S100A8 are known to recruit MDSCs from bone marrow to the peripheral blood and tumor microenvironment.[28–33] Additionally, S100A8/9 protein has been reported to inhibit the differentiation of MDSCs into DCs.[33] We also demonstrated that 5-FU suppressed the protein expression levels of Bv8 and S100A8 protein in AB1-HA cells (Figure 4E,F). In addition, we observed that 3LL cells treated with S-1 (in vivo) displayed a substantial reduction in Bv8, S100A8, and iNOS, whereas 5-FU treatment (in vitro) suppressed the gene expression of Bv8 (Figure S4A,B). Taken together, these results suggested that fluoropyrimidines decreased tumor-infiltrating MDSCs by inhibiting the secretion of tumor cell-derived mediators.

3.4 | The expression of Bv8 and S100A8 in tumor cells was essential for tumor growth and MDSC accumulation

To further ascertain the important function of Bv8 and S100A8 in the tumor microenvironment, we suppressed the expression of Bv8 and S100A8 in AB1-HA cells by shRNA. The cell proliferation of AB1-HA cells was not affected by the transfection with non-targeting control plasmid (control shRNA), Bv8-targeting shRNA plasmid (Bv8 shRNA), and S100A8-targeting shRNA plasmid (S100A8 shRNA) in vitro (Figure S5). Thus, we evaluated the effects of Bv8 or S100A8 gene-silencing on tumor development and MDSC recruitment in vivo. The tumor volume and number of MDSCs in the tumor and spleen were examined and compared to those in mice treated with

S-1 (Figure 5). The knockdown of the Bv8 gene in AB1-HA cells resulted in delayed tumor progression (Figure 5A) and a decrease in MDSCs in both spleen and tumor tissue specimens (Figure 5B,C) as well as in S-1-treated mice. S100A8 knockdown in tumor cells also suppressed tumor development (Figure 5D) and MDSC infiltration (Figure 5E,F). Additionally, the knockdown of the Bv8 or S100A8 expression in AB1-HA cells enhanced the number of CD8+ TILs (Figure S6A,B). These data indicated that tumor-derived Bv8 and S100A8, which were downregulated by S-1, play an essential role in the recruitment of immunosuppressive myeloid cells. Bv8 and S100A proteins have been known to promote the recruitment of hematopoietic cells from bone marrow to peripheral blood.[28–33] These results support the hypothesis that tumor-derived Bv8 and S100A8 were dominant regulators of MDSC recruitment not only in tumor tissue but peripheral blood.

3.5 | Combination therapy with S-1 enhanced the antitumor efficacy of ICIs through the regulation of MDSCs

Considering the immunomodulatory effects of fluoropyrimidines, we next investigated the efficacy of combination immunotherapy with S-1 and ICIs in thoracic tumors. AB1-HA tumor-bearing mice were treated with S-1 and/or anti-PD-1 antibodies. Even though monotherapy significantly suppressed tumor development, combination therapy with S-1 and anti-PD-1 antibodies showed superior tumor-suppressive effects (Figure 6A). Flow cytometry showed that S-1 monotherapy or combined treatment induced a significant decrease in MDSCs in the tumor and spleen, whereas anti-PD-1 antibody monotherapy had no such effects (Figure 6B). Interestingly, the combined treatment with S-1 and anti-PD-1 antibody synergistically amplified the number of CD8+ TILs in tumors (Figure 6C), with even more CD4+ and CD8+ T cells detected in the spleen (Figure S7A,B).

Regarding the standard therapy for NSCLC patients, combination immunotherapy with ICIs and platinum-doublet chemotherapy including PEM or taxane have been approved.[6,7] Therefore, we investigated whether the addition of CBDCA to S-1 and anti-PD-1 antibody combination treatment could improve the synergistic therapeutic efficacy in vivo. Although CBDCA monotherapy significantly inhibited tumor growth, S-1 monotherapy or combined S-1 + CBDCA therapy demonstrated the tendency to have superior tumor-suppressive effects through the reduction of MDSCs in both the spleen and tumor (Figure S8A,B). Also, we found that the addition of CBDCA to S-1 dramatically decreased the growth of subcutaneous tumors and the number of infiltrating MDSCs (Figure S8C,D). These results indicated that combination immunotherapy with platinum and S-1 had the potential to induce antitumor immune responses more efficiently than the current standard regimens in thoracic cancer.

To support our hypothesis that S-1 is the optimal chemotherapeutic agent in combination therapy with ICIs, we further examined the synergistic therapeutic efficacy of the administration of S-1 and
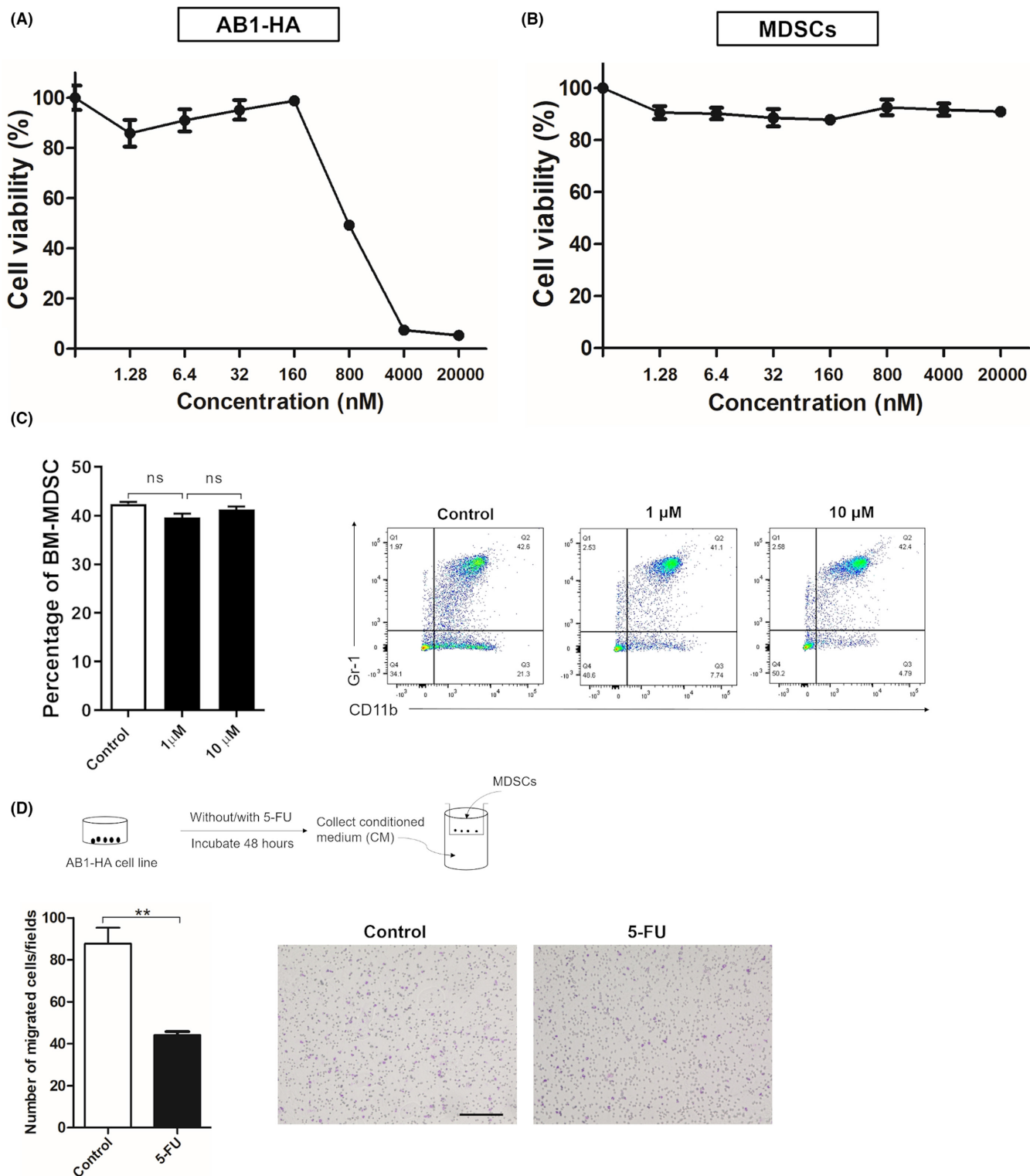
FIGURE 3 Fluoropyrimidines suppress the MDSC-accumulating capacity of tumor cells. (A) The cytotoxic effect of 5-FU on AB1-HA cells was determined by MTT assay. (B) The cytotoxic effect of 5-FU on mouse spleen-derived MDSCs was analyzed using a cell counting kit. (C) Flow cytometry of the differentiation of mouse bone marrow-derived MDSCs in vitro ($n = 3$). Bone marrow cells were collected from AB1-HA tumor-bearing mice and co-cultured with or without 5-FU, 10 ng/ml GM-CSF and 10 ng/ml IL-4 and 0.2 ng/ml TGF-β. (D) Representative images and the quantitative evaluation of the migrated mouse MDSCs in vitro. Mouse splenic MDSCs were observed in the upper chamber, and those that migrated toward the lower chamber were stained. The lower chamber contained AB1-HA cells cultured with or without 5-FU ($n = 3$). Scale bar: 200 μm. Data are shown as the mean ± SEM. ***$p < 0.001$; **$p < 0.01$; ns, not statistically significant by Mann–Whitney U-test or a one-way ANOVA.
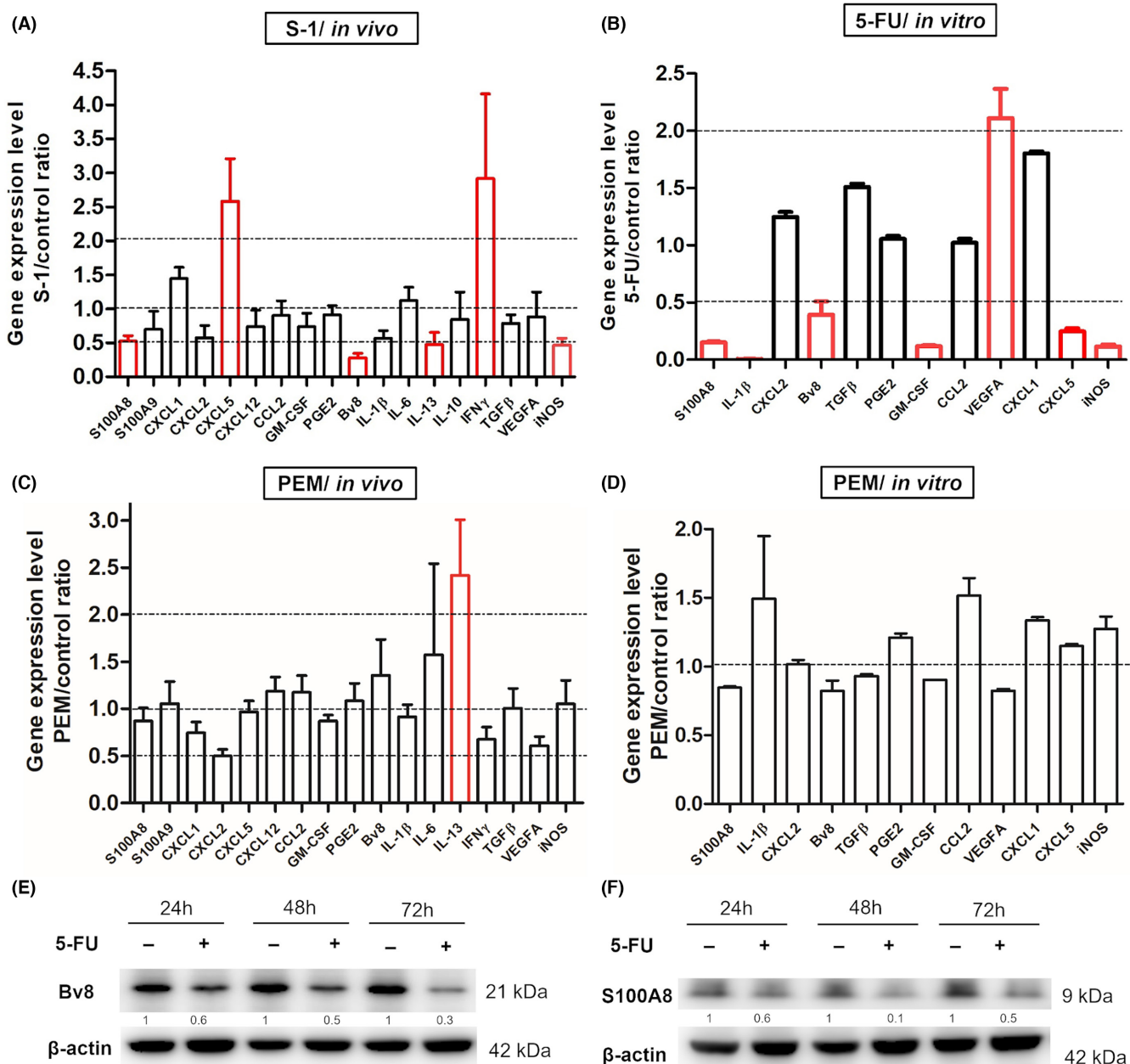
FIGURE 4 Fluoropyrimidines downregulate the tumor-derived Bv8 and S100A8. (A) Comparison of the mRNA expression levels of MDSC-related cytokines in AB1-HA tumor tissue treated with or without S-1. (B) The gene expression levels of AB1-HA cells treated with 5-FU (IC50, 1 μM) for 48h in vitro. (C) Comparison of the gene expression levels of MDSC-related cytokines in AB1-HA tumor tissue treated with or without PEM. (D) The mRNA expression levels of MDSC-related cytokines in AB1-HA cells treated with PEM (IC50, 54nM) for 48h in vitro. Fold changes in the mRNA expression of the treatment groups in comparison with the control group are shown. Genes upregulated more than two-fold or downregulated lower than half in treatment groups in comparison with the control group are shown as red columns. (E, F) The protein expression levels of Bv8 (E) and S100A8 (F) in AB1-HA cells treated with 5-FU (1 μM) for 24–72h. The ratio of target protein per β-actin was indicated.

CBDCA and/or anti-PD-1 antibodies. Although anti-PD-1 mono-therapy was less effective on day 21, combination therapy with PD-1 blockade and CBDCA plus S-1 suppressed the tumor development and MDSC recruitment (Figure S8E,F). In addition, we also compared the synergistic effects of combination immunotherapy with CBDCA+S-1+anti-PD-1 antibody with the current standard regimen in NSCLC: combination therapy with CBDCA+PEM+PD-1 blockade (Figure 6D). Interestingly, combination therapy with

CBDCA+S-1+anti-PD-1 antibody showed superior antitumor effects to the current standard regimen. Combination immunotherapy with S-1 showed superiority in the reduction of MDSCs and the enhancement of TILs in comparison with the regimen with PEM (Figure 6E,F and Figure S7B). Thus, our findings demonstrated that combination therapy consisting of S-1, but not PEM, with ICI therapy could further enhance antitumor immune responses by preventing the infiltration of MDSCs.
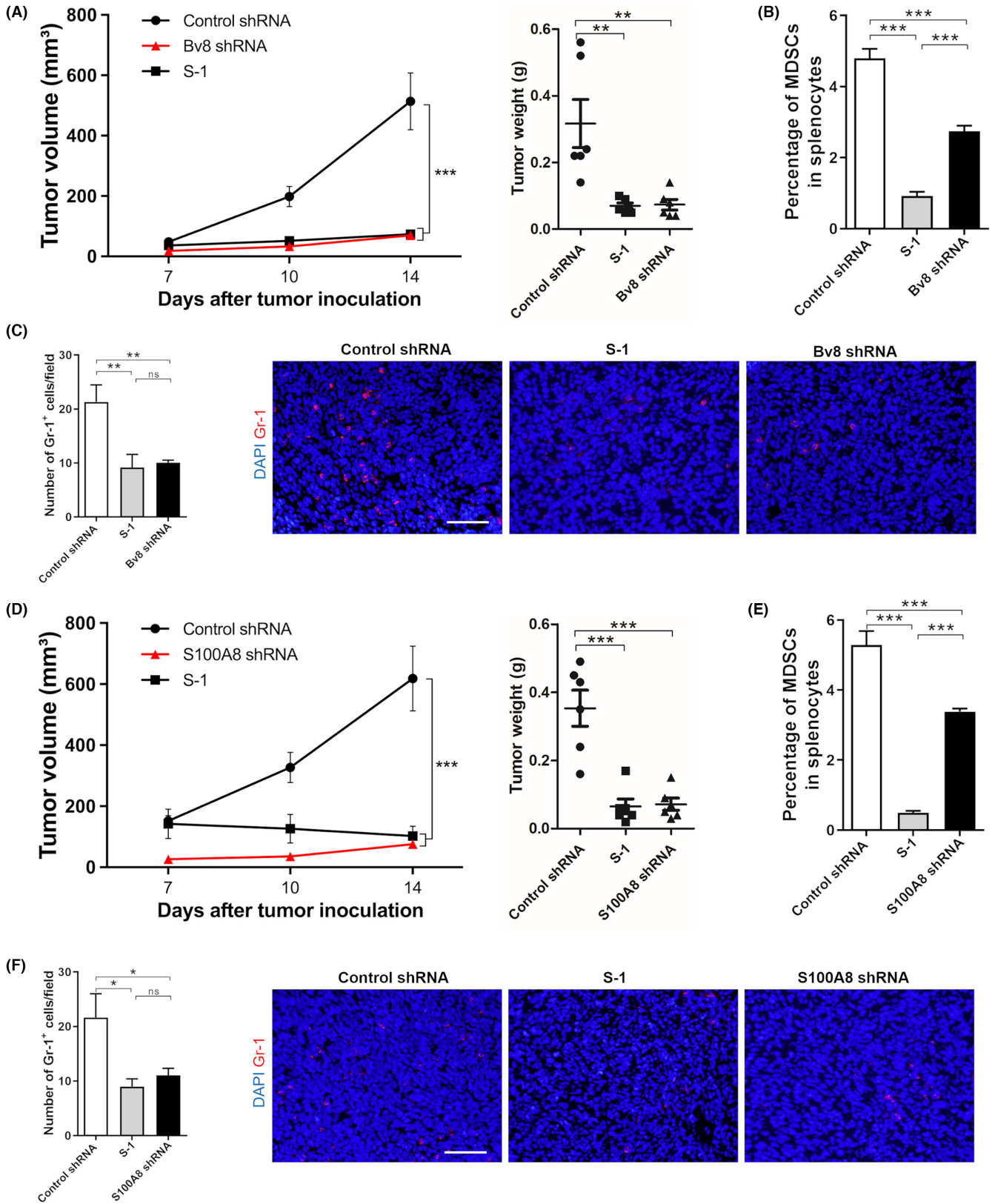
4 | DISCUSSION

Several clinical studies have investigated the efficacy of S-1 in advanced NSCLC. Okamoto and colleagues elucidated the clinical benefit of combination therapy with CBDCA plus S-1 in a phase III study.[34] We previously conducted clinical trials to evaluate the efficacy and safety of S-1-containing regimens as a first-line therapy for elderly NSCLC patients[35] or NSCLC patients with interstitial lung disease.[36] Additionally, our preclinical study indicated that S-1 suppressed the progression of MPM.[23] These studies highlighted S-1 as

FIGURE 5 Knockdown of tumor-derived Bv8 or S100A8 inhibits tumor growth and the accumulation of MDSCs. (A) The evaluation of the volume and the weight in AB1-HA tumor tissue transfected with non-targeting control plasmid (control shRNA) or Bv8-targeting shRNA plasmid (Bv8 shRNA) in vivo. Tumor-bearing mice were treated with daily oral gavage S-1 (8.3 mg/kg/day) or vehicle from day 7 to 13 after tumor inoculation. (B) Flow cytometry of CD11b$^+$Gr-1$^+$ MDSCs in spleen derived from each group in (A). (C) Representative images and quantitative evaluation of the number of Gr-1$^+$ cells per field in tumor tissue specimens of the AB1-HA tumor-bearing mice in (A). Scale bar, 200 μm. (D) The evaluation of the volume and the weight of AB1-HA tumor tissue transfected with non-targeting control plasmid (control shRNA) or S100A8-targeting shRNA plasmid (S100A8 shRNA) in vivo. Tumor-bearing mice were treated with daily oral gavage S-1 (8.3 mg/kg/day) or vehicle from day 7 to 13 after tumor inoculation. (E) Flow cytometry of CD11b$^+$Gr-1$^+$ MDSCs in spleen derived from each group in (D). (F) Representative images and the quantitative evaluation of Gr-1$^+$ cells per field from tumor tissues of the AB1-HA tumor-bearing mice in (D). Scale bar, 200 μm. Data are shown as the mean ± SEM. ***$p < 0.001$; **$p < 0.01$; *$p < 0.05$; ns, not statistically significant by Mann–Whitney U-test or a one-way ANOVA.

a well tolerated, effective option for a broad range of patients with thoracic tumors.

In the present study, among the cytotoxic chemotherapeutic agents approved for patients with thoracic tumors, we demonstrated that 5-FU and S-1 significantly reduced tumor-associated MDSCs. In contrast, the contributions of PEM to the elimination of MDSCs were limited, even though combination immunotherapy with PEM, platinum, and PD-1 blockade are approved for NSCLC patients.[6] Furthermore, our study revealed that combination therapy with S-1, CBDCA, and anti-PD-1 antibodies resulted in superior antitumor effects in comparison with PEM-containing therapy in vivo. These results indicated that S-1 has the potential to provide a major advance with respect to recent combination immunotherapy for thoracic tumors. In particular, the clinical benefits of combination therapy with cytotoxic agents and ICIs remain unclear in MPM, even though the Checkmate 743 study elucidated that combined therapy with anti-PD-1 and anti-CTLA-4 antibodies prolonged the overall survival of MPM patients.[37] The present study also raised the possibility of combination immunotherapy with S-1 as a promising therapeutic option to overcome MPM.

Recent preclinical studies demonstrated that several cytotoxic antitumor reagents, for example, GEM[38,39] or 5-FU,[16,17] eliminated tumor-associated MDSCs. However, the mechanisms through which cytotoxic reagents selectively deplete MDSCs in the tumor microenvironment have been unclear. We revealed the tumor-dependent mechanism through which fluoropyrimidines suppress the recruitment of MDSCs. Our previous study revealed that continuous treatment with CDDP and PEM reduced tumor-infiltrating MDSCs and improved the antitumor efficacy of PD-1 blockade via the regulation of tumor-derived vascular endothelial growth factor A (VEGFA).[40] In contrast, S-1 did not regulate the VEGFA expression in tumor tissue in the present study. To investigate the therapeutic targets of S-1, we focused on tumor cell-derived Bv8 and S100A8 as key mediators of the accumulation of MDSCs.

Bv8 has been identified as a secreted protein that belongs to a peptide with five-disulfide-bridge motif.[29,30] In addition to its proangiogenic functions, Bv8 has been known to contribute to the mobility of myeloid cells, including MDSCs.[30] S100A8 and S100A9 are known as calcium-binding proteins that form a heterodimer (S100A8/9).[31–33] Recent studies elucidated the pivotal roles of S100A8/9 in the recruitment of MDSC. Sinha and colleagues[31] demonstrated that MDSCs expressed carboxylated N-glycan receptors, which bind to

S100A8/9. Therefore, Bv8 and S100A8/9 have attracted attention as the key factors for determining tumor progression via the regulation of MDSCs.[28,30,32] A recent study identified the expression of Bv8 as a prognostic biomarker of human colorectal carcinoma.[41] In addition, the serum concentration of S100A8/9 protein was identified as a prognostic biomarker in advanced melanoma patients treated with anti-PD-1 antibodies.[42] Regarding thoracic tumors, Huang and colleagues investigated the expression of S100A8/9 in tumor tissue from NSCLC patients.[43] They proposed S100A8/9 as a possible prognostic biomarker because its expression level was correlated with tumor differentiation. Taken together, tumor-derived Bv8 and S100A8/9 were presumed to be promising therapeutic targets in solid tumors. In the present study, we demonstrated the importance of tumor-derived Bv8 and S100A8 in tumor progression and the recruitment of MDSCs by performing gene-silencing in tumor cells. Furthermore, our findings revealed that S-1 treatment downregulates the expression of multiple MDSC-related mediators, including Bv8 and S100A8. The antitumor effects of neutralizing anti-Bv8 or anti-S100A8 antibodies have been elucidated in several preclinical studies.[44,45] We therefore concluded that S-1 should effectively improve antitumor immunity as a multiple inhibitor for MDSC-related mediators.

Our findings indicated that S-1 increased the number of DCs in tumor tissue. DCs have been known to play pivotal roles in the antitumor immune response as principal antigen-presenting cells.[46] The recruitment and activation of DCs have been investigated as a critical target in cancer immunotherapy. Moreover, recent studies have suggested that MDSCs have the potential to differentiate into DCs at tumor sites.[27] In this study, S-1 downregulated the expression of tumor-derived S100A8, which inhibited the differentiation of MDSCs into DCs as a heterodimer S100A8/9.[33] Thus, we believed that the drastic effects of S-1 on tumor-infiltrating MDSCs were partially based on the facilitation of differentiation of MDSCs into DCs.

The present study was associated with some limitations. First, we only demonstrated the impact of S-1 in combination immunotherapy in preclinical models. To assess the potential of S-1 as a novel option for cancer immunotherapy in thoracic tumors, further clinical studies are required. Considering the pivotal role of tumor-derived Bv8 and S100A8 in our preclinical model, the serum levels of Bv8 and S100A8 are presumed to determine the clinical benefit in thoracic tumor patients treated with ICIs or S-1. The accumulation of this clinical evidence should support combination immunotherapy with S-1
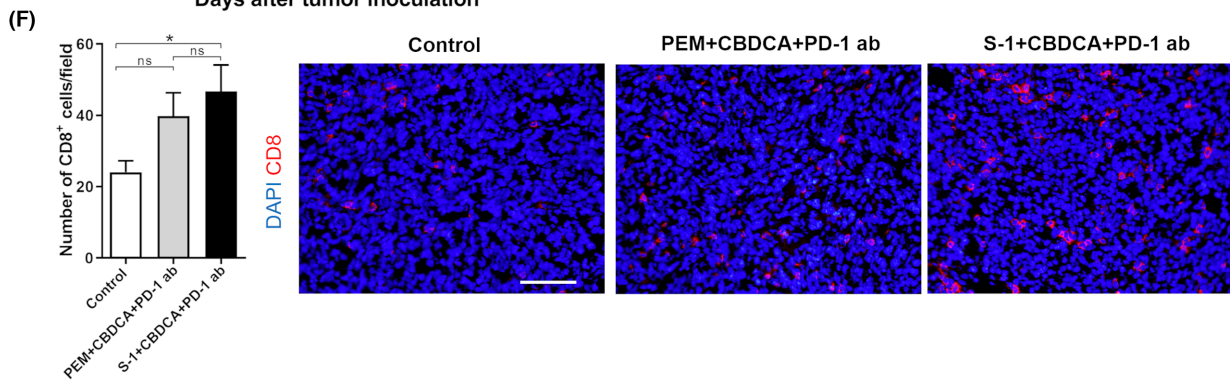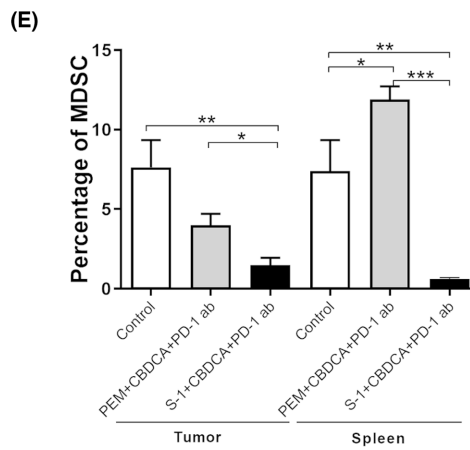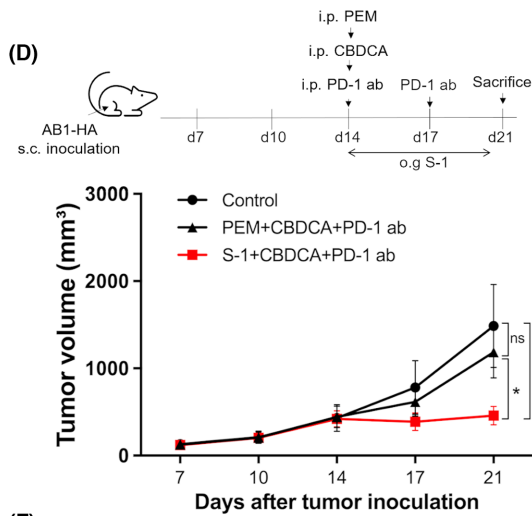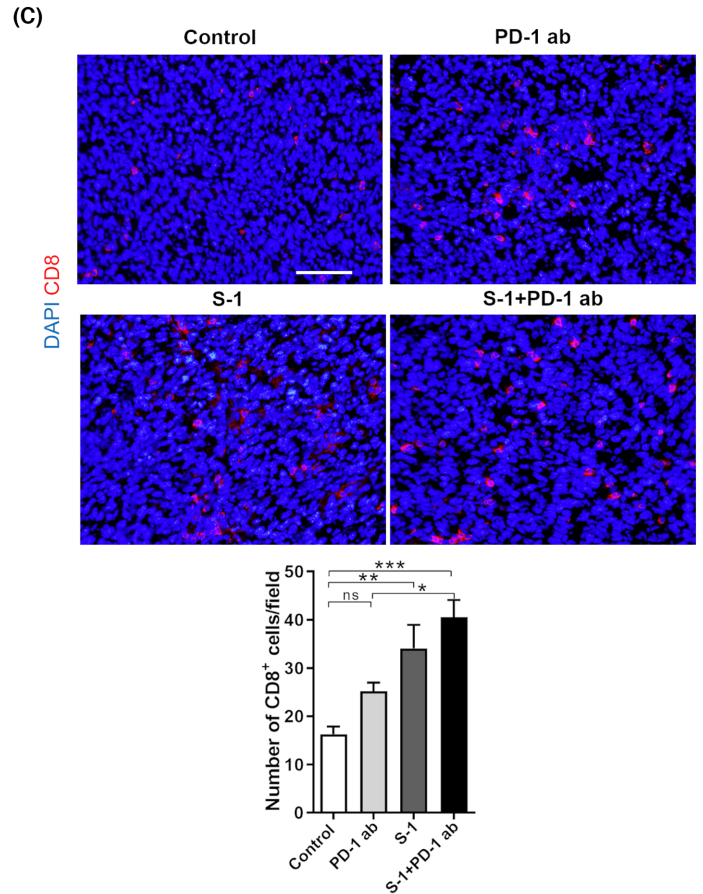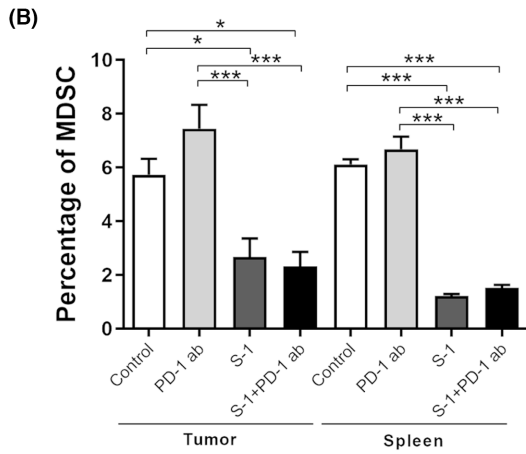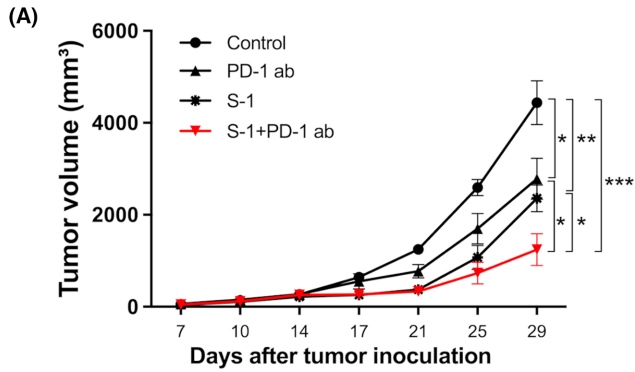
FIGURE 6 Combination therapies with S-1 enhance the antitumor efficacy of PD-1 blockade. (A) The evaluation of the tumor volume of AB1-HA tumor-bearing mice treated with anti-PD-1 antibodies on days 7 and 17 after tumor cell injection. Mice were treated with S-1, which was administered by daily oral gavage from day 14 to day 20 after tumor inoculation or combined therapy with PD-1 antibodies. (B) Flow cytometry of $CD11b^+Gr-1^+$ MDSCs in tumor tissue and spleen on day 21 from AB1-HA tumor-bearing mice treated with PD-1 antibodies and/or S-1 ($n = 6$ per group). (C) Representative images and the quantitative evaluation of the number of $CD8a^+$ cells in tumor tissue studied in (B) ($n = 5$ per group). (D) The treatment schedule and evaluation of the tumor volume of AB1-HA tumor-bearing mice treated with S-1+CBDCA+PD-1 antibodies or PEM+CBDCA+PD-1 antibodies ($n = 6$ per group). (E) Flow cytometry of $CD11b^+ Gr-1^+$ MDSCs in tumor tissue and spleen on day 21 from the AB1-HA tumor-bearing mice in (D). (F) Representative images and quantitative evaluation of the number of $CD8a^+$ cells in tumor tissue specimens in (D). Scale bar, 200 μm. Data are shown as the mean ± SEM. ***$p < 0.001$; **$p < 0.01$; *$p < 0.05$; ns, not statistically significant by Mann–Whitney U-test or a one-way ANOVA.

for thoracic tumors. Second, the mechanisms through which fluoro-pyrimidines suppressed the expression of Bv8 and S100A8 in tumor cells have not been sufficiently explained. Recent studies elucidated that the expression of Bv8 and S100A8 was induced by phosphorylation of STAT3.[33,47,48] In addition, 5-FU has been demonstrated to suppress the phosphorylation of STAT3 in tumor cells.[49] These results raised the hypothesis that S-1 suppresses tumor-derived Bv8 and S100A8 via the regulation of STAT3 signaling. Additional analyses are needed to reveal the detailed mechanisms.

Our findings revealed that S-1 depletes tumor-infiltrating MDSCs via the downregulation of tumor-derived Bv8 and S100A8. Furthermore, S-1-containing regimens improved the efficacy of ICI in a preclinical model. The present study provides an important rationale to develop novel combined immunotherapy for patients with thoracic tumors.

DISCLOSURE

Hirokazu Ogino, Hiroshi Nokihara, and Yasuhiko Nishioka reports research fees paid from Taiho Pharmaceutical Co., Ltd.

ETHICS STATEMENT

Approval of the research protocol by an Institutional Reviewer Board: N/A.

Informed Consent: N/A.

Registry and the Registration No. of the study/trial: N/A.

Animal Studies: All experimental protocols were reviewed and approved by the animal research committee of The University of Tokushima, Japan (approved number T30-130).

ORCID

Yasuhiko Nishioka https://orcid.org/0000-0001-6311-1654

REFERENCES

1. Sirri E, Kieschke J, Vohmann C, et al. Survival of malignant mesothelioma and other rare thoracic cancers in Germany and the United States: a population-based study. *Int J Cancer.* 2020;147(6):1548-1558. doi:10.1002/ijc.32931
2. Siegel RL, Miller KD, Fuchs HE, Jemal A. Cancer statistics, 2022. *CA Cancer J Clin.* 2022;72(1):7-33. doi:10.3322/caac.21708
3. Sun L, Zhang L, Yu J, et al. Clinical efficacy and safety of anti-PD-1/PD-L1 inhibitors for the treatment of advanced or metastatic cancer: a systematic review and meta-analysis. *Sci Rep.* 2020;10(1):1-13. doi:10.1038/s41598-020-58674-4
4. Gong J, Chehrazi-Raffle A, Reddi S, Salgia R. Development of PD-1 and PD-L1 inhibitors as a form of cancer immunotherapy: a comprehensive review of registration trials and future considerations. *J Immunother Cancer.* 2018;6(1):1-18. doi:10.1186/s40425-018-0316-z
5. Chen RL, Zhou JX, Cao Y, et al. The efficacy of PD-1/PD-L1 inhibitors in advanced squamous-cell lung cancer: a meta-analysis of 3112 patients. *Immunotherapy.* 2019;11(17):1481-1490. doi:10.2217/imt-2019-0101
6. Gandhi L, Rodríguez-Abreu D, Gadgeel S, et al. Pembrolizumab plus chemotherapy in metastatic non-small-cell lung cancer. *N Engl J Med.* 2018;378:2078-2092. doi:10.1056/NEJMoa1801005
7. Socinski MA, Jotte RM, Cappuzzo F, et al. Atezolizumab for first-line treatment of metastatic nonsquamous NSCLC. *N Engl J Med.* 2018;378(24):2288-2301. doi:10.1056/NEJMoa1716948
8. Park SM, Youn JI. Role of myeloid-derived suppressor cells in immune checkpoint inhibitor therapy in cancer. *Arch Pharm Res.* 2019;42(7):560-566. doi:10.1007/s12272-019-01165-6
9. Ortiz ML, Lu L, Ramachandran I, Gabrilovich DI. Myeloid-derived suppressor cells in the development of lung cancer. *Cancer Immunol Res.* 2014;2(1):50-58. doi:10.1158/2326-6066.cir-13-0129
10. Monu NR, Frey AB. Myeloid-derived suppressor cells and anti-tumor T cells: a complex relationship. *Immunol Investig.* 2012;41(6-7):595-613. doi:10.3109/08820139.2012.673191
11. Fares CM, Allen EMV, Drake CG, Allison JP, Hu-Lieskovan S. Mechanisms of resistance to immune checkpoint blockade: why does checkpoint inhibitor immunotherapy not work for all patients? *Am Soc Clin Oncol Educ Book.* 2019;39:147-164. doi:10.1200/EDBK_240837
12. Peranzoni E, Ingangi V, Masetto E, Pinton L, Marigo I. Myeloid cells as clinical biomarkers for immune checkpoint blockade. *Front Immunol.* 2020;11(7):1-24. doi:10.3389/fimmu.2020.01590

13. Kim HR, Park SM, Seo SU, et al. The ratio of peripheral regulatory T cells to Lox-1+ polymorphonuclear myeloid-derived suppressor cells predicts the early response to anti-PD-1 therapy in patients with non-small cell lung cancer. *Am J Respir Crit Care Med*. 2019;199(2):243-246. doi:10.1164/rccm.201808-1502LE

14. Kitano S, Postow MA, Ziegler CGK, et al. Computational algorithm-driven evaluation of monocytic myeloid-derived suppressor cell frequency for prediction of clinical outcomes. *Cancer Immunol Res*. 2014;2(8):812-821. doi:10.1158/2326-6066.CIR-14-0013

15. Sangaletti S, Ferrara R, Tripodo C, Garassino MC, Colombo MP. Myeloid cell heterogeneity in lung cancer: implication for immunotherapy. *Cancer Immunol Immunother*. 2021;70(9):2429-2438. doi:10.1007/s00262-021-02916-5

16. Otsubo D, Yamashita K, Fujita M, et al. Early-phase treatment by low-dose 5-fluorouracil or primary tumor resection inhibits MDSC-mediated lung metastasis formation. *Anticancer Res*. 2015;35(8):4425-4432.

17. Vincent J, Mignot G, Chalmin F, et al. 5-Fluorouracil selectively kills tumor-associated myeloid-derived suppressor cells resulting in enhanced T cell-dependent antitumor immunity. *Cancer Res*. 2010;70(8):3052-3061. doi:10.1158/0008-5472.CAN-09-3690

18. Fukushima M. S-1 review from preclinical pharmacology. *Gastric Cancer*. 2009;12(SUPPL. 1):3-9. doi:10.1007/s10120-008-0488-1

19. Shirasaka T. Development history and concept of an oral anticancer agent S-1 (TS-1®): its clinical usefulness and future vistas. *Jpn J Clin Oncol*. 2009;39(1):2-15. doi:10.1093/jjco/hyn127

20. Takeda K. Clinical development of S-1 for non-small cell lung cancer: a Japanese perspective. *Ther Adv Med Oncol*. 2013;5(5):301-311. doi:10.1177/1758834013500702

21. Totani Y, Saito Y, Hayashi M, et al. A phase II study of S-1 monotherapy as second-line treatment for advanced non-small cell lung cancer. *Cancer Chemother Pharmacol*. 2009;64(6):1181-1185. doi:10.1007/s00280-009-0981-1

22. Takechi T, Nakano K, Uchida J, et al. Antitumor activity and low intestinal toxicity of S-1, a new formulation of oral tegafur, in experimental tumor models in rats. *Cancer Chemother Pharmacol*. 1996;39(3):205-211. doi:10.1007/s002800050561

23. Van TT, Hanibuchi M, Kakiuchi S, et al. The therapeutic efficacy of S-1 against orthotopically implanted human pleural mesothelioma cells in severe combined immunodeficient mice. *Cancer Chemother Pharmacol*. 2011;68(2):497-504. doi:10.1007/s00280-010-1503-x

24. Aston WJ, Hope DE, Nowak AK, Robinson BW, Lake RA, Lesterhuis WJ. A systematic investigation of the maximum tolerated dose of cytotoxic chemotherapy with and without supportive care in mice. *BMC Cancer*. 2017;17(1):1-10. doi:10.1186/s12885-017-3677-7

25. Annels NE, Shaw VE, Gabitass RF, et al. The effects of gemcitabine and capecitabine combination chemotherapy and of low-dose adjuvant GM-CSF on the levels of myeloid-derived suppressor cells in patients with advanced pancreatic cancer. *Cancer Immunol Immunother*. 2014;63(2):175-183. doi:10.1007/s00262-013-1502-y

26. Yang Z, Guo J, Weng L, Tang W, Jin S, Ma W. Myeloid-derived suppressor cells – new and exciting players in lung cancer. *J Hematol OncolJ Hematol Oncol*. 2020;13(1):10. doi:10.1186/s13045-020-0843-1

27. Marvel D, Gabrilovich DI. Myeloid-derived suppressor cells in the tumor microenvironment: expect the unexpected. *J Clin Invest*. 2015;125(9):3356-3364. doi:10.1172/JCI80005

28. Shojaei F, Ferrara N. Refractoriness to antivascular endothelial growth factor treatment: role of myeloid cells. *Cancer Res*. 2008;68(14):5501-5504. doi:10.1158/0008-5472.CAN-08-0925

29. Shojaei F, Singh M, Thompson JD, Ferrara N. Role of Bv8 in neutrophil-dependent angiogenesis in a transgenic model of cancer progression. *Proc Natl Acad Sci USA*. 2008;105(7):2640-2645. doi:10.1073/pnas.0712185105

30. LeCouter J, Zlot C, Tejada M, Peale F, Ferrara N. Bv8 and endocrine gland-derived vascular endothelial growth factor stimulate hematopoiesis and hematopoietic cell mobilization. *Proc Natl Acad Sci USA*. 2004;101(48):16813-16818. doi:10.1073/pnas.0407697101

31. Sinha P, Okoro C, Foell D, Freeze HH, Ostrand-Rosenberg S, Srikrishna G. Proinflammatory S100 proteins regulate the accumulation of myeloid-derived suppressor cells. *J Immunol*. 2008;181(7):4666-4675. doi:10.4049/jimmunol.181.7.4666

32. Azizian-Farsani F, Abedpoor N, Sheikhha MH, Gure AO, Nasr-Esfahani MH, Ghaedi K. Receptor for advanced glycation end products acts as a fuel to colorectal cancer development. front. *Front Oncol*. 2020;10:552283. doi:10.3389/fonc.2020.552283

33. Cheng P, Corzo CA, Luetteke N, et al. Inhibition of dendritic cell differentiation and accumulation of myeloid-derived suppressor cells in cancer is regulated by S100A9 protein. *J Exp Med*. 2008;205(10):2235-2249. doi:10.1084/jem.20080132

34. Okamoto I, Yoshioka H, Morita S, et al. Phase III trial comparing Oral S-1 plus carboplatin with paclitaxel plus carboplatin in chemotherapy-naïve patients with advanced non-small-cell lung cancer: results of a West Japan oncology group study. *J Clin Oncol*. 2010;28(36):5240-5246. doi:10.1200/JCO.2010.31.0326

35. Goto H, Okano Y, Machida H, et al. Phase II study of tailored S-1 monotherapy with a 1-week interval after a 2-week dosing period in elderly patients with advanced non-small cell lung cancer. *Respir Investig*. 2018;56(1):80-86. doi:10.1016/j.resinv.2017.09.003

36. Hanibuchi M, Kakiuchi S, Atagi S, et al. A multicenter, open-label, phase II trial of S-1 plus carboplatin in advanced non-small cell lung cancer patients with interstitial lung disease. *Lung Cancer*. 2018;125:93-99. doi:10.1016/j.lungcan.2018.09.007

37. Baas P, Scherpereel A, Nowak AK, et al. First-line nivolumab plus ipilimumab in unresectable malignant pleural mesothelioma (CheckMate 743): a multicentre, randomised, open-label, phase 3 trial. *Lancet*. 2021;397(10272):375-386. doi:10.1016/S0140-6736(20)32714-8

38. Le HK, Graham L, Cha E, Morales JK, Manjili MH, Bear HD. Gemcitabine directly inhibits myeloid derived suppressor cells in BALB/c mice bearing 4T1 mammary carcinoma and augments expansion of T cells from tumor-bearing mice. *Int Immunopharmacol*. 2009;9(7-8):900-909. doi:10.1016/j.intimp.2009.03.015

39. Wu C, Tan X, Hu X, Zhou M, Ding C, Alerts E. Tumor microenvironment following gemcitabine treatment favors differentiation of immunosuppressive Ly6C high myeloid cells. *J Immunol*. 2020;204(1):212-223. doi:10.4049/jimmunol.1900930

40. Otsuka K, Mitsuhashi A, Goto H, et al. Anti-PD-1 antibody combined with chemotherapy suppresses the growth of mesothelioma by reducing myeloid-derived suppressor cells. *Lung Cancer*. 2020;146(5):86-96. doi:10.1016/j.lungcan.2020.05.023

41. Yoshida Y, Goi T, Kurebayashi H, Morikawa M, Hirono Y, Katayama K. Prokineticin 2 expression as a novel prognostic biomarker for human colorectal cancer. *Oncotarget*. 2018;9(53):30079-30091. doi:10.18632/oncotarget.25706

42. Wagner NB, Weide B, Gries M, et al. Tumor microenvironment-derived S100A8/A9 is a novel prognostic biomarker for advanced melanoma patients and during immunotherapy with anti-PD-1 antibodies. *J Immunother Cancer*. 2019;7(1):343. doi:10.1186/s40425-019-0828-1

43. Huang H, Huang Q, Tang T, et al. Clinical significance of calcium-binding protein S100A8 and S100A9 expression in non-small cell lung cancer: S100A8 and S100A9 expression in NSCLC. *Thorac Cancer*. 2018;9(7):800-804. doi:10.1111/1759-7714.12649

44. Shojaei F, Wu X, Zhong C, et al. Bv8 regulates myeloid-cell-dependent tumour angiogenesis. *Nature*. 2007;450(7171):825-831. doi:10.1038/nature06348

45. Hiratsuka S, Watanabe A, Aburatani H, Maru Y. Tumour-mediated upregulation of chemoattractants and recruitment of myeloid cells predetermines lung metastasis. *Nat Cell Biol*. 2006;8(12):1369-1375. doi:10.1038/ncb1507

46. Wculek SK, Cueto FJ, Mujal AM, Melero I, Krummel MF, Sancho D. Dendritic cells in cancer immunology and immunotherapy. *Nat Rev Immunol*. 2020;20(1):7-24. doi:10.1038/s41577-019-0210-z

47. Xin H, Lu R, Lee H, et al. G-protein-coupled receptor agonist BV8/prokineticin-2 and STAT3 protein form a feed-forward loop in both normal and malignant myeloid cells. *J Biol Chem*. 2013;288(19):13842-13849. doi:10.1074/jbc.M113.450049

48. Qu X, Zhuang G, Yu L, Meng G, Ferrara N. Induction of Bv8 expression by granulocyte colony-stimulating factor in CD11b^{+}Gr1^{+} cells: key role of Stat3 signaling. *J Biol Chem*. 2012;287(23):19574-19584. doi:10.1074/jbc.M111.326801

49. Yang Y, Ma L, Xu Y, et al. Enalapril overcomes chemoresistance and potentiates antitumor efficacy of 5-FU in colorectal cancer by suppressing proliferation, angiogenesis, and NF-κB/STAT3-regulated proteins. *Cell Death Dis*. 2020;11(6):477. doi:10.1038/s41419-020-2675-x

SUPPORTING INFORMATION

Additional supporting information can be found online in the Supporting Information section at the end of this article.

How to cite this article: Nguyen NT, Mitsuhashi A, Ogino H, et al. S-1 eliminates MDSCs and enhances the efficacy of PD-1 blockade via regulation of tumor-derived Bv8 and S100A8 in thoracic tumor. *Cancer Sci*. 2023;114:384-398. doi: 10.1111/cas.15620